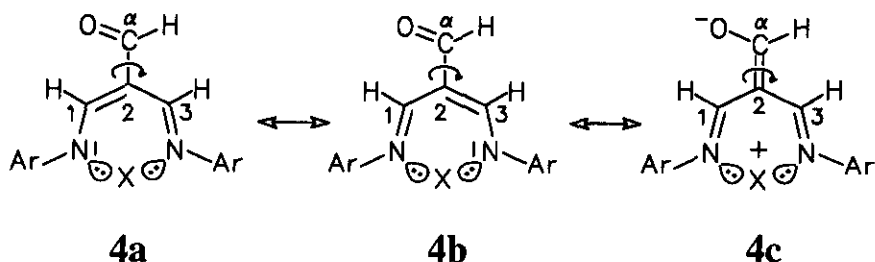


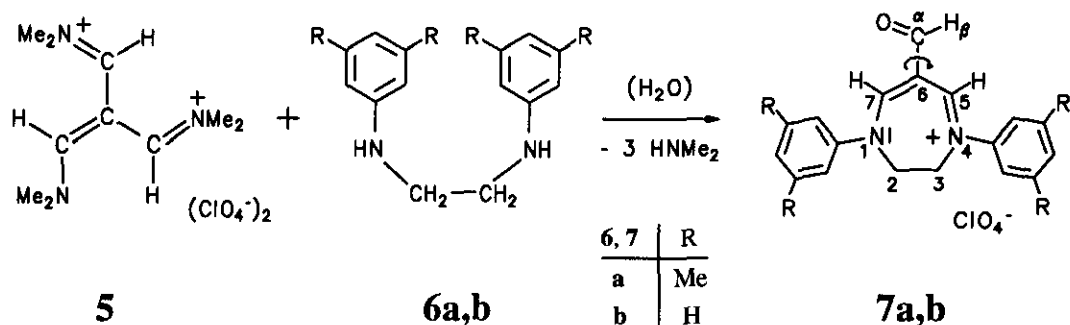
To quantify the characteristic π -electron donor property in the electronic ground state, we envisaged vinamidine derivatives (**4a**) with the formyl group as a π -acceptor substituent at the reactive position C(2). This heterocyclic array ensures equivalence of the two X-N bonds, which would not be possible with acyclic forms (1). A vinamidinium cation will be formed for $X = (\text{CH}_2\text{CH}_2)^+$ in **4a**, whereas a vinamidinide anion would result formally in **4a** for chelate complexes of divalent metals M with $X = 0.5 \text{ M(II)}$. These models have fixed and comparable geometries, in contrast to the parent compound with $X = \text{H}$ which is useless for the present purpose due to its extended geometry⁶ shown later in **8** with a hydrogen bond perturbing the formyl group. The *m*-dimethylated *N*-aryl groups in **4a** (and **8**) were chosen for greater stability and solubility of the substances.



Although the two resonance formulae (**4a,b**) are nearly degenerate, their 1-/3-H atoms and all other twin substituents remain non-equivalent (diastereotopic) until the formyl substituent rotates into a perpendicular orientation. However, a strong π donation into the formyl group would stabilize the coplanar orientation because it implies a significant contribution of formula (**4c**) to the ground state. Thus the following criteria might be expected to provide more or less quantitative evidence for the π -donor quality of the vinamidine systems as depending on the nature of X: (i) Structurally, the formyl substituent should prefer to remain coplanar with the vinamidine, with a shortened bond C(2)-C(α) and an lengthened carbonyl bond. (ii) The latter perturbation of the formyl group might be discernable from infrared wave numbers and intensities. (iii) Energetically, the π interaction should be expressed as a retarded formyl rotation about the partial double bond C(2)-C(α) in **4a-c**.

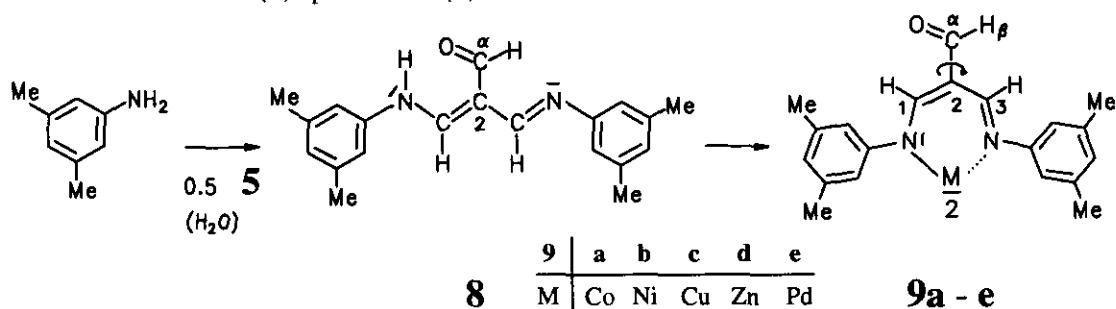
SYNTHESES AND STRUCTURES OF THE MODEL COMPOUNDS

Considering aldehyde syntheses in view of the sluggish formylation of a vinamidinium cation⁶ and the low reactivity of 2,3-dihydro-1,4-diaryl-1,4-diazepinium salts (**3**) in general,⁵ we preferred to use 1,2-dianilinoethane⁷ (**6b**) and to prepare⁷ its tetramethyl derivative (**6a**) for condensations^{8,9} with Arnold's bis(perchloro-



rate)¹⁰ (5). The two 1,4-diaryl-6-formyl-2,3-dihydro-1,4-diazepinium perchlorates (7a) (the more soluble one) and (7b) were found to be totally stable³ in the absence of bases. Their solid-state structures could not be determined, but their spectroscopic properties were sufficiently similar to those¹¹⁻¹⁴ of structurally known analogs¹⁵⁻¹⁸ to certify the constitution.

The 2-formylvinamidine (8) was also prepared from Arnold's salt¹⁰ (5) much more efficiently than by formylation.⁶ The non-equivalence⁶ of its two 3,5-dimethylaniline parts was confirmed by low temperature ¹³C-nmr spectra. The chelate complexes (9a-e) were easily formed from 8 or its hydrogenperchlorate. Their crystal structures determined by X-ray analyses excluded the possibility of *N,O* rather than *N,N* chelation and allowed us to compare the geometries of the complexes (9a-9d) in a complete series with increasing numbers of 3d electrons from 3d⁷ Co(II) up to 3d¹⁰ Zn(II).



The solid-state structures of 9a-d shown in Figures 1 - 4 are characterized by only one element of molecular symmetry, a C₂ axis containing the metal center and passing through the midpoints of the N(1)-N(1') and N(2)-N(2') distances. Therefore, all of them are chiral; as each one of these single crystals was centrosymmetric and thus composed of both enantiomers, the M (minus)¹⁹ antipodes were arbitrarily depicted in the Figures. This description may be gleaned most easily from the C(4)-O and C(4')-O' orientations about the chirality axes C(4)-C(4').

The chelate "bite" distances N(1)-N(2) in Table 1 (Entry 1) are smaller than that in the 6-cyclopropyl-2,3-dihydro-1,4-diphenyl-1,4-diazepinium perchlorate (3.206 Å)¹⁵ by only about 10%. The remaining four edges (Entries 2-4) of the ligating tetrahedra (the *N* atoms) are longer than the "bites", but the nature of the pseudo-tetrahedral distortions will become more directly clear from bond angle comparisons (Table 2). As all of the chelate bite angles N(1)-M-N(2) are much smaller (Entry 20) than the tetrahedral value 109.5°, the coordination tetrahedra in 9a-d are always elongated rather than compressed. This is one of the factors which in the molecular orbital approximation^{20,21} may cause the 3d orbitals of π symmetry to become the energetically highest (SOMOs). The smallest of the remaining (exocyclic) angles (Entries 21-24), N(2)-M-N(2') in Entry 22, is close to the tetrahedral value in 9a, 9b and 9d but decreases even further toward the value for planar coordination in 9c (Figure 3) by twisting. The 3,5-dimethylanilino groups attached to these N(2) and N(2') atoms tend to come correspondingly close (Entry 17) and to arrange themselves face-to-face. Of course, the degree of such digonal twisting may also be read from the dihedral angles in Table 3 (Entry 38) between the planes M-N(1)-N(2) and M-N(1')-N(2'). Without the formyl and the *N*-aryl substituents, Co (9a) and Ni (9b) as well as Zn (9d) would have a symmetry close to D_{2d}, whereas Cu (9c) would reside in a milieu approximating D₂ symmetry (corresponding to the expected Jahn-Teller distortion). The actual symmetry reduction

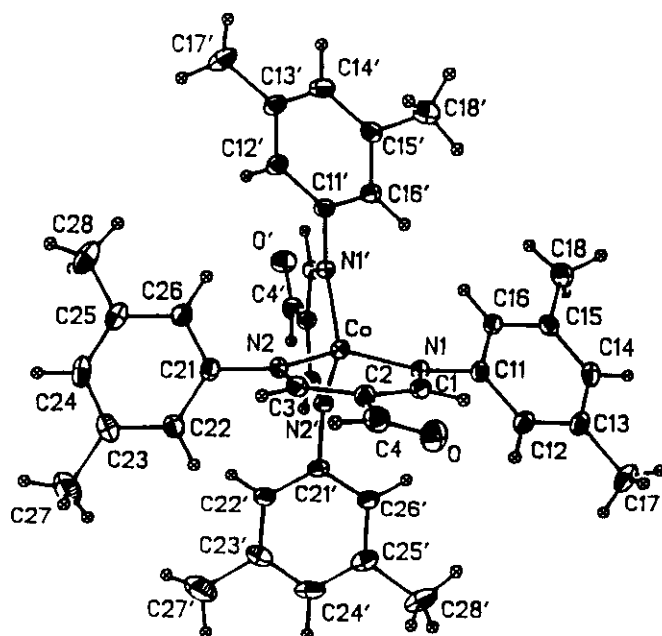


Figure 1. Structure of the Co(II) bis(chelate) (9a) with 20% ellipsoids, seen nearly along the axis of chirality

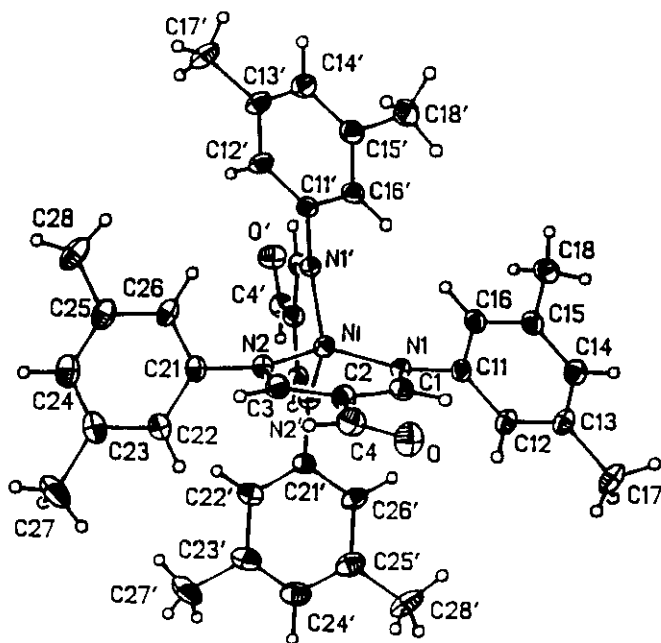


Figure 2. Structure of the Ni(II) bis(chelate) (9b) with 20% ellipsoids, seen nearly along the axis of chirality

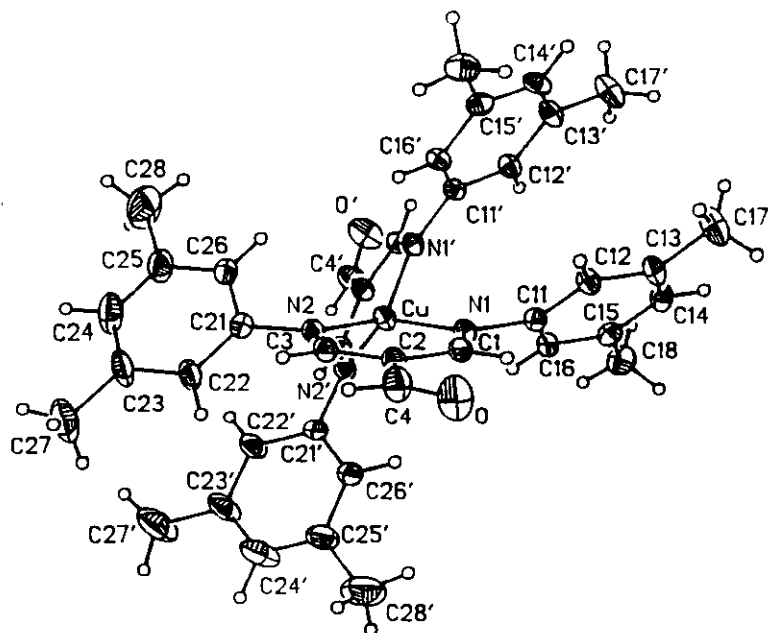


Figure 3. Structure of the Cu(II) bis(chelate) (9c) with 20% ellipsoids, seen nearly along the axis of chirality

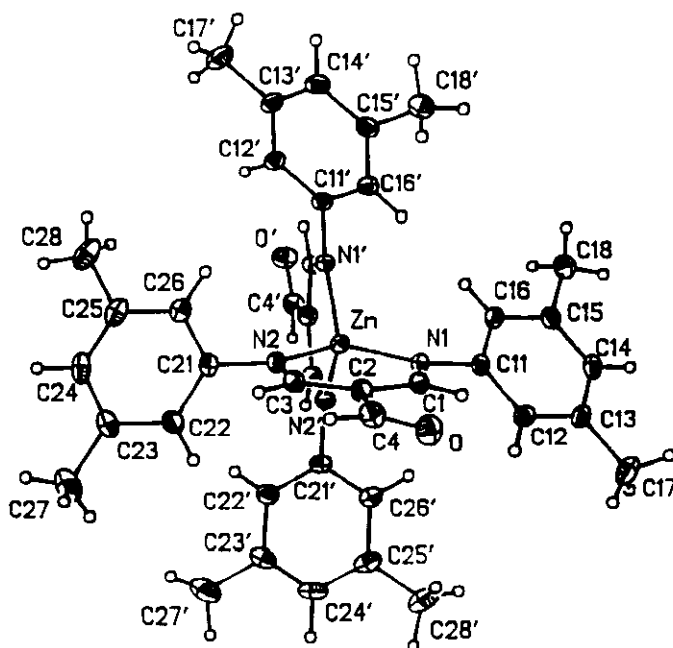


Figure 4. Structure of the Zn(II) bis(chelate) (9d) with 20% ellipsoids, seen nearly along the axis of chirality

Table 1. Bonded and non-bonded distances (Å) in the chelate complexes (9a-d) (C₂ symmetry, pseudotetrahedral), and averaged values for 9e (planar coordination)^a

Entry	Distances	Co (9a)	Ni (9b)	Cu (9c)	Zn (9d)	Pd (9e)
1	bite N(1)-N(2)	2.955	2.864	2.875	2.987	2.80(7)
2	edge N(1)-N(1')	3.467	3.476	3.075	3.509	2.87(2)
3	edge N(2)-N(2')	3.236	3.197	2.985	3.260	3.02(2)
4	edge N(1)-N(2')	3.310	3.303	3.606	3.337	(trans)
5	depth M-C(2)	3.229	3.270	3.267	3.232	3.23(2)
6	bond M-N(1)	1.972(3)	1.953(4)	1.950(4)	1.989(3)	2.03(2)
7	bond M-N(2)	1.965(4)	1.943(4)	1.953(4)	1.987(3)	2.04(2)
8	bond N(1)-C(1)	1.309(4)	1.321(5)	1.309(6)	1.310(4)	1.30(3)
9	bond N(2)-C(3)	1.307(4)	1.321(5)	1.299(7)	1.306(4)	1.29(3)
10	bond C(1)-C(2)	1.401(5)	1.392(6)	1.411(7)	1.405(4)	1.39(4)
11	bond C(2)-C(3)	1.408(5)	1.394(5)	1.395(7)	1.405(4)	1.40(5)
12	bond C(2)-C(4)	1.434(5)	1.442(5)	1.442(8)	1.441(4)	1.45(4)
13	bond C(4)-O	1.230(4)	1.225(5)	1.196(7)	1.224(4)	1.24(3)
14	bond N(1)-C(11)	1.432(4)	1.426(5)	1.433(6)	1.427(4)	1.44(3)
15	bond N(2)-C(21)	1.429(4)	1.431(5)	1.428(7)	1.429(4)	1.44(3)
16	<i>ipso</i> C(11)-C(11')	4.761	4.737	3.257	4.803	2.97(1)
17	<i>ipso</i> C(21)-C(21')	4.009	3.910	3.276	4.030	3.01(7)
18	<i>para</i> C(14)-C(14')	8.494	8.416	4.883	8.526	4.7 (2)
19	<i>para</i> C(24)-C(24')	6.952	6.828	5.595	6.967	4.7 (2)

^a M = metal; in column 9e read N(4) for N(1'), N(3) for N(2'), C(41) for C(11'), C(31) for C(21'), C(44) for C(14'), and C(34) for C(24').

to C₂ is also expressed by longitudinal inflexion as a third kind of pseudotetrahedral distortion, since C(2)-M-C(2') differs from 180° (Entry 25) such that these atoms cannot be simultaneously located on the axis of chirality.

The opposing chelate heterocycles in 9a-d are equivalent by C₂ symmetry. Their independent bond lengths C-C (Entries 10, 11) and N-C (Entries 8, 9 and 14, 15) are equal within the error limits, in accord with the resonance formulation (4a-c). Each heterocycle is practically planar: Torsional angles in Table 3 along the chelate periphery (Entries 39-44) reveal the slight boat-like distortions. The intra-annular angles C(1)-C(2)-C(3) of 9a-d (Entry 34) are effectively equal (=125°) and only marginally smaller than that of the diazepinium salt (128.5°)¹⁵ mentioned above. A consequence of this angular opening at C(2) is increased steric repulsion of the conformationally flexible formyl oxygen atoms. Nevertheless, the C(4)-O carbonyl groups are almost perfectly coplanar with the chelate heterocycles, as seen from the torsional angles (Entries 45-47) and in Figures 1 - 4. Conformationally maximized π conjugation in the sense of 4c is an obvious reason for this, pointing to a strong π -donor character of the heterocycle. However, the expected shortening of the C(2)-C(4) bond lengths

Table 2. Bond angles and longitudinal inflexion ($^{\circ}$) in the chelate complexes (**9a-d**) (C_2 symmetry, pseudotetrahedral), and averaged values for **9e** (planar coordination) ^a

Entry	Angle		Co (9a)	Ni (9b)	Cu (9c)	Zn (9d)	Pd (9e)
20	N(1)-M-N(2)	bite	97.3(1)	94.7(1)	94.9(2)	97.4(1)	87.2(7)
21	N(1)-M-N(1')	edge	123.1(2)	125.7(2)	104.1(2)	123.8(1)	91.4(7)
22	N(2)-M-N(2')	edge	110.9(2)	110.7(2)	99.7(2)	110.3(1)	94.4(7)
23	N(1)-M-N(2')	edge	114.4(1)	115.9(1)	135.1(2)	114.1(1)	177.3(8)
24	N(2)-M-N(1')	edge	114.4(1)	115.9(1)	135.1(2)	114.2(1)	176.7(8)
25	C(2)-M-C(2')	^b	173.7(3)	171.4(3)	174.2(3)	172.4(3)	169
26	M-N(1)-C(1)		120.9(2)	123.5(3)	123.4(3)	120.4(2)	120(2)
27	M-N(2)-C(3)		121.7(2)	124.6(2)	123.7(3)	121.0(2)	120(2)
28	M-N(1)-C(11)		121.3(2)	119.7(2)	119.6(3)	121.5(2)	121(4)
29	M-N(2)-C(21)		119.6(2)	117.9(2)	117.1(3)	119.8(2)	121(5)
30	C(1)-N(1)-C(11)		117.3(3)	116.4(3)	117.0(4)	117.6(2)	119(5)
31	C(3)-N(2)-C(21)		118.2(3)	117.1(3)	119.0(4)	118.7(2)	119(7)
32	N(1)-C(1)-C(2)		127.6(3)	126.6(3)	126.8(4)	127.7(3)	126(5)
33	N(2)-C(3)-C(2)		126.7(3)	125.6(4)	127.2(5)	127.2(3)	126(3)
34	C(1)-C(2)-C(3)		125.6(3)	124.8(3)	123.6(5)	126.1(3)	121(3)
35	C(1)-C(2)-C(4)		117.6(3)	118.3(3)	119.3(5)	117.0(3)	120(7)
36	C(3)-C(2)-C(4)		116.7(3)	116.8(4)	117.1(5)	116.7(3)	117(9)
37	C(2)-C(4)-O		126.2(3)	125.6(4)	126.4(5)	126.1(3)	122(6)

^a M = metal; in column **9e** read N(4) for N(1'), N(3) for N(2'), C(41) for C(11'), C(31) for C(21'), C(44) for C(14'), and C(34) for C(24'). - ^b Inflexion; in column **9e** read C(52) for C(2').

Table 3. Selected torsional angles ($^{\circ}$) in the chelate complexes (**9a-e**) ^a

Entry	Angle	Co (9a)	Ni (9b)	Cu (9c)	Zn (9d)	Pd (9e)
38	dihedral	88.6	89.1	62.4	88.5	178.5
39	N(2)-M-N(1)-C(1)	-0.3(3)	-1.4(3)	+5.1(4)	+0.2(2)	-41(2)
40	M-N(1)-C(1)-C(2)	-2.6(5)	-1.5(6)	-2.5(7)	-3.2(4)	+20(4)
41	N(1)-C(1)-C(2)-C(3)	+5.1(6)	+4.2(7)	-2.1(8)	+5.8(5)	+18(4)
42	C(1)-C(2)-C(3)-N(2)	-3.9(6)	-3.1(7)	+2.1(9)	-4.7(5)	-18(4)
43	C(2)-C(3)-N(2)-M	+0.7(5)	-0.6(5)	+2.4(8)	+1.3(4)	-19(4)
44	C(3)-N(2)-M-N(1)	+1.2(3)	+2.3(3)	-5.1(4)	+0.7(2)	+41(2)
45	N(1)-C(1)-C(2)-C(4)	-179.1(3)	-179.5(4)	+179.3(5)	-178.8(3)	+177(2)
46	N(2)-C(3)-C(2)-C(4)	+179.8(3)	+179.4(4)	-179.2(5)	+179.9(3)	-178(2)
47	C(1)-C(2)-C(4)-O	-2.1(6)	-2.9(6)	-2.4(9)	-1.4(5)	-14(4)

^a M = metal; values for **9e** averaged from two independent molecules.

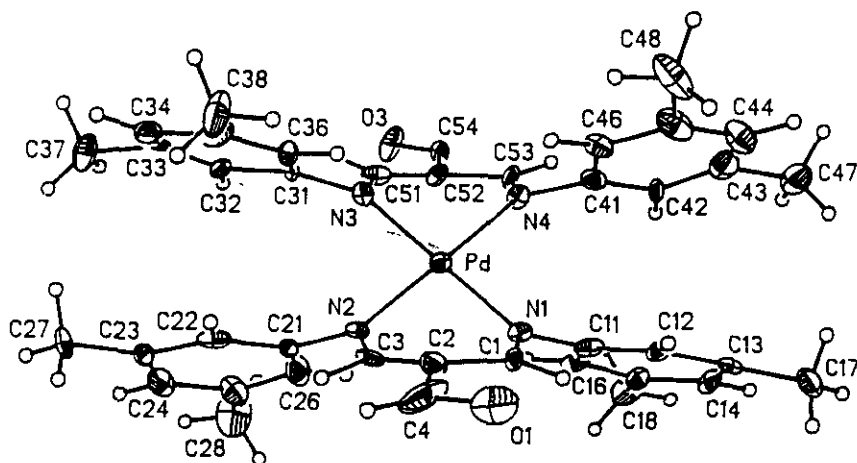


Figure 5. Structure of the Pd(II) bis(chelate) (**9e**) with 20% ellipsoids, seen almost parallel to the vinamidine planes

and elongations of the C(4)-O double bonds are not borne out in Table 1, since the values (Entries 12, 13) are approximately normal.²²

The palladium chelate (**9e**) shows a spatially different coordination sphere in Figure 5. All four N atoms are perfectly coplanar with their ligand atoms and form a common coordination plane containing the Pd atom. The latter plane makes angles of $\approx 35^\circ$ with both vinamidine moieties NCCCN, which are therefore arranged in an almost parallel fashion but stepped by 1.6 Å. The whole structure exhibits a rough approximation to S_2 symmetry (compare Entry 25), with Pd as the center of inversion. However, this crystal contained a second independent molecule which had much larger vibration ellipsoids for its oxygen atoms than shown for O(1) in Figure 5. Since the crystal was destroyed after the centrosymmetrical part of the data collection had been recorded, the results of this structure determination were of minor quality but sufficiently reliable. Hence, we report the geometrical data of **9e** as averages over both ligands in both independent molecules, excluding some atoms which vibrate more strongly at the periphery. The formyl substituents C(4)-O(1) and C(54)-O(3) are a little less coplanar with respect to the vinamidine planes (Entries 45-47). This appears to be related to a more halfboat-like (yet internally almost symmetric) shape of these heterocycles with a small lift of C(2) (Entries 41, 42) and a strong one of Pd (Entries 39, 44 and 40, 43). Although not too much significance should be assigned to the numerical data, we notice a decreased angle C(1)-C(2)-C(3) (Entry 34) as a major response in the heterocycle to the compressed "bite" (Entry 1) and bite angle (Entry 20). Despite such differences, the formyl groups in **9a-e** are all attached at C(2) in the same distance from the metal centers (see Entry 5).

SPECTROSCOPIC ANALYSES

For the pseudotetrahedral chelate complexes (**9a-d**), the infrared (ir) spectra in KBr were very similar even in the fingerprint regions. The aldehyde vibration with its well-separated and strong ir absorption should be suitable for determinations of ir intensities which are expected²³ to measure resonance interactions. Applying re-

commended^{24,25} techniques (see Experimental), we have observed the integrated absorption intensities E in Table 4 for resonances of the formyl groups of **7a** and **9a-e** in solution (typically 0.027 M). Even the 2,3-dihydro-1,4-diazepinium salt (**7a**) (but not **7b**) was sufficiently soluble in 1,1,2,2-tetrachloroethane (as in CHCl_3). Ir intensities of polycarbonyl compounds are said to behave additively²⁶ and to be not coupled across the central metal²⁷ in chelate complexes. Therefore, as the bis(chelates) (**9a-e**) carry two formyl groups, their E values were computed per chelate unit, that is, for the half-molecules. There is a definite trend in the series (Entry 49), and the total region is comparable with that of simple carbonyl intensities,^{24,25} but the averaged value is equal to that for **7a**. Hence the global charge of the vinamidine system has no effect because the presence or absence of a metal ion is obviously not sensed in this case. Similar failures of intensity/substituent correlation are known.²⁸ On the other hand, the wave numbers ν (Entry 48) of **9a-e** are strongly decreased and indicate enhanced π donation, as expected for the vinamidinide character, whereas the vinamidinium system of **7a** does not cause a shift of the aldehyde absorption from the usual region.

Table 4. Molar integral ir absorptions E at ir wave numbers ν of the formyl groups, and activation parameters (ΔH^\ddagger , E_a , ΔS^\ddagger , $\lg A$, ΔG^\ddagger) of formyl rotation for the 2,3-dihydro-1,4-diazepinium perchlorate (**7a**)^a and the chelate complexes (**9a-e**) in 1,1,2,2-tetrachloroethane- d_2 solution

Entry	Quantity	7a ^a	Co (9a)	Ni (9b)	Cu (9c)	Zn (9d)	Pd (9e)
48	ir: ν (cm^{-1})	1703	1653	1653	1653	1656	1648
49	$10^3 \cdot E$ (b)	8.4 (5)	10.5 (5)	9.6 (5)	7.5 (5)	7.5 (5)	6.8 (5)
50	nmr: ΔH^\ddagger (c)	12.4 (4)	-	14 (1)	-	16.0 (3)	17.4 (4)
51	E_a (c)	12.9 (4)	-	14 (1)	-	16.6 (3)	18.0 (4)
52	ΔS^\ddagger (d)	+5 (2)	-	-3 (5)	-	+1.4 (9)	+5 (1)
53	$\lg A$	14.1 (3)	-	13 (1)	-	13.6 (2)	14.4 (3)
54	ΔG^\ddagger (e)	11.0 (1)	14.8 (2)	14.71 (3)	-	15.53 (1)	15.80 (1)

^a Ir (Entries 48, 49) measured in $\text{C}_2\text{H}_2\text{Cl}_4$, ^1H nmr (Entries 50-54) in acetone- d_6 /DMSO- d_6 (5:1). -

^b ($\text{l}\cdot\text{mol}^{-1}\cdot\text{cm}^{-2}$). - ^c (kcal/mol). - ^d ($\text{cal}\cdot\text{mol}^{-1}\cdot\text{K}^{-1}$). - ^e (kcal/mol , at $+32^\circ\text{C}$).

If the central metal ions were able to compete with the formyl substituent for the π electrons of the vinamidine, this might result in diminished intensities E and increased wave numbers ν because the contribution of resonance hybrid (**4c**) would become smaller. Such π electron attraction, if any, would be expected to run parallel to the deficiency of 3d (or 4d) electrons with π -symmetry properties, perhaps in the progression from Zn ($3d^{10}$) and Pd (planar $4d^8$) over Cu ($3d^9$) and Ni ($3d^8$) to Co ($3d^7$). The observed ir trends are just opposed for intensities E in **9a-e** and vanishingly small for wave numbers ν (which were also not useful for similar but octahedral chelate complexes²⁷). We conclude that other factors dominate the ir properties. However, the expectations are borne out by careful analyses of the temperature-dependent ^1H nmr spectra as follows.

With a coplanar formyl orientation, the NCH protons (5-/7-H or 1-/3-H) in **7a**, **9d** (Zn) and **9e** (Pd) are diastereotopic (non-equivalent), and their nmr signals split into widely separated singlets at sufficiently low temperatures. The chemical shift differences $\Delta\delta = 0.43$, ca. 0.56 (slightly temperature-dependent), and 0.40, respec-

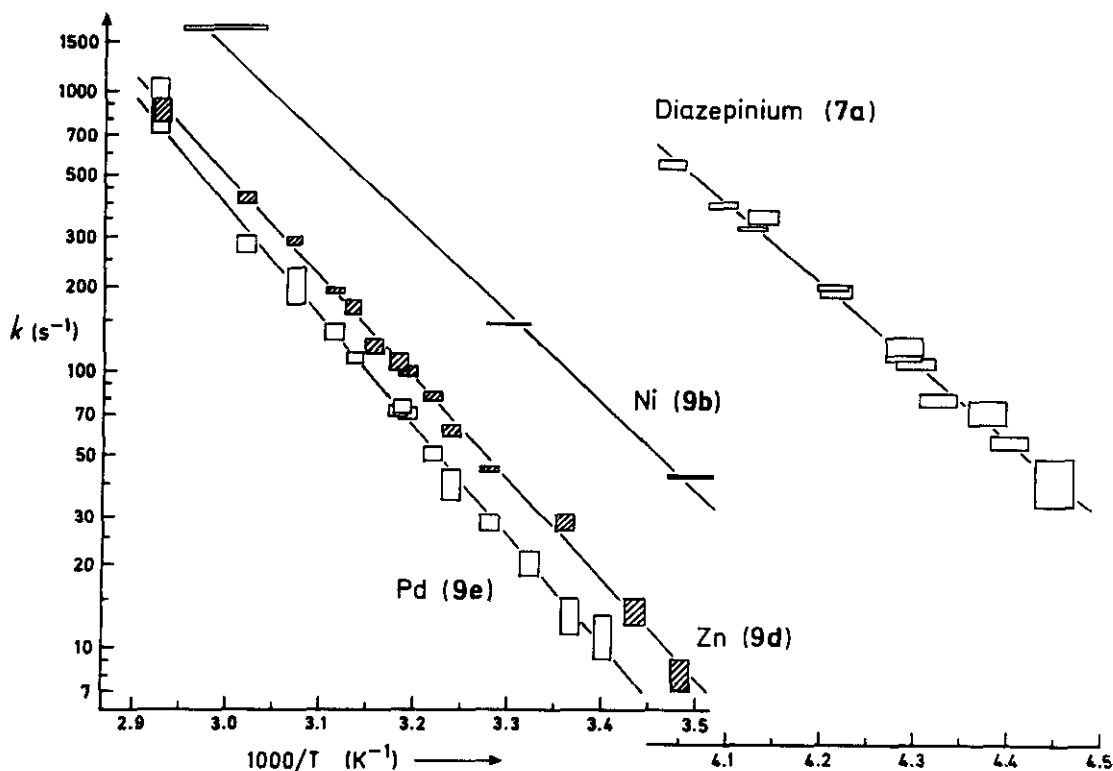


Figure 6. Arrhenius plots for formyl rotation in **7a**, in paramagnetic **9b** (Ni), and in the diamagnetic chelates (**9d**) (Zn, hatched symbols) and (**9e**) (Pd)

tively, in these diamagnetic compounds are of such a magnitude that they can be explained only by a differentiating influence of a neighbouring formyl group (like in benzaldehyde²⁹), but not across the metal centre. Hence, the formyl conformations appear to be similar to those in the crystals of **9d** and **9e**. Formyl rotation became fast on the nmr time scale at +25°C for **7a** only, with fully coalesced signals in the ¹H and ¹³C nmr spectra. The temperature-dependent rate constants were computed by total lineshape analyses³⁰ and are shown in Figure 6. These data led to the activation parameters for formyl rotation in Table 4. Ring inversion as described¹⁴ for related salts was also noticed by ¹H nmr non-equivalence of 2-/3-CH₂ (C₂ symmetry) but did not interfere.

The chelates with Co (**9a**) and Ni (**9b**) ions are paramagnetic and required a different treatment. Although the very unusual ¹H nmr chemical shifts of **9b** span the range from $\delta = -12$ to +375 ppm and are strongly temperature-dependent, they could be assigned unequivocally by comparisons with the less soluble analog³¹ of **9b** (lacking the methyl groups) and with further vinamidine chelates.³² Every kind of protons in **9b** (two unpaired electron spins) experiences an individual paramagnetically induced shift (taken relative to the diamagnetic Zn chelate (**9d**) in this work) which is inversely proportional to the absolute temperature (Curie law). It is therefore convenient^{32,33} to convert these values into "reduced shifts" δ (see Experimental) which are normally

independent of the temperature within the error limits. Figure 7b demonstrates this for most of the protons in **9b**. The exception is the formyl proton (β) whose δ values decrease on heating because the less coplanar conformations become more populated. Furthermore, *all* other proton resonances are seen to be split in pairs (intensity ratio 1:1) and to merge pairwise above individual coalescence temperatures T_C . Since lineshape analyses were not feasible due to the general paramagnetic line-broadening, which was expressed by the error bars in Figure 7, we have read the T_C values (see Experimental) from the diagram and used the extrapolated ^1H nmr frequency differences $\Delta\nu$ to compute the rate constants $k_C = \pi\cdot\Delta\nu/(2)^{0.5}$ at the three most suitable coalescence temperatures. The resultant activation parameters from Figure 6 were included in Table 4 for **9b**. A corresponding treatment was not possible for the Cu bis(chelate) (**9c**) due to its unresolved ^1H nmr spectrum.

The Co bis(chelate) (**9a**) was analyzed in the same way, but its strongly broadened ^1H nmr resonances allowed to detect the diastereotopic splitting only for the relatively narrow *p*-H signals (Figure 7a). The temperature-dependent δ of formyl (β) points to rotation again, but compared with **9b** (Ni in Figure 7b) the δ values are much more negative for 1-/3-H and β -H yet more positive for CH_3 and *p*-H. This is due to the third unpaired spin on tetrahedral Co(II) and a larger magnetic anisotropy. Hence, formyl rotation in **9a** could be characterized by merely one k_C value (see Experimental) at a single T_C and by the ΔG^\ddagger parameter derived from it (Table 4); but the closely similar structures of **9a** and **9b** (Figures 1 and 2) suggest that the activation entropy should be approximately zero for both.

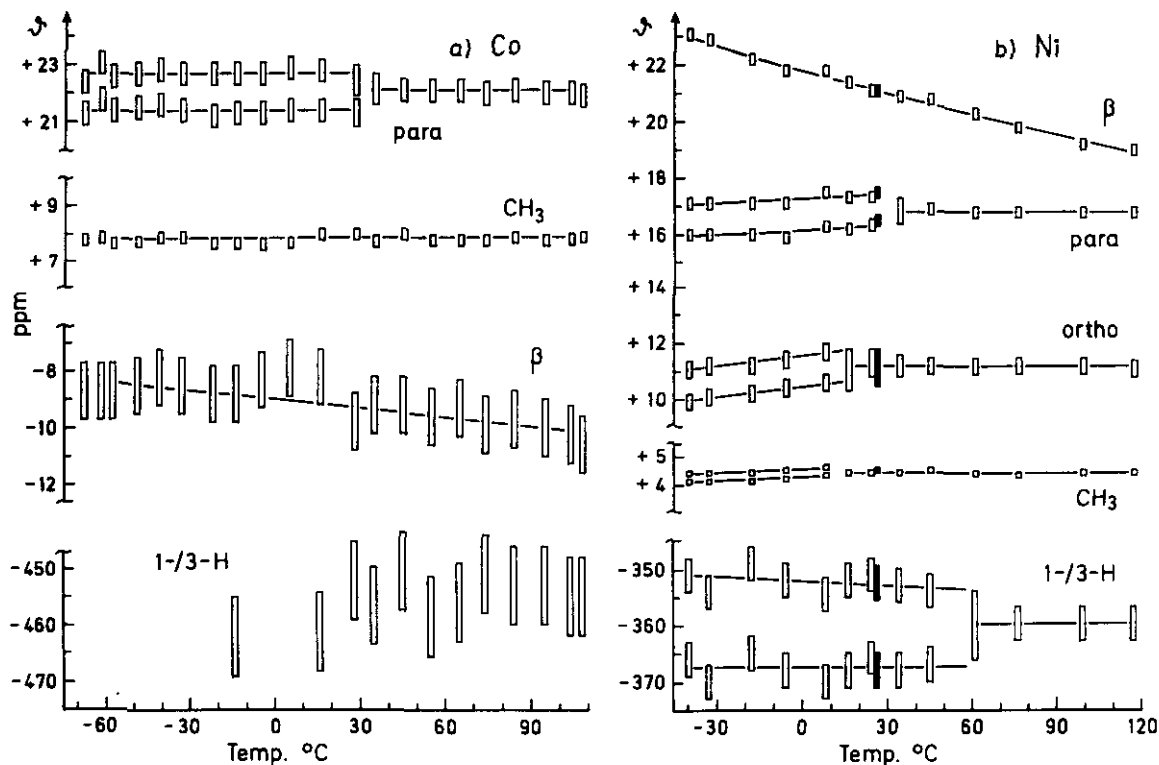
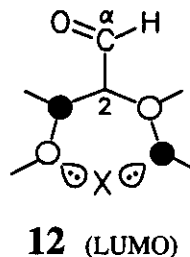
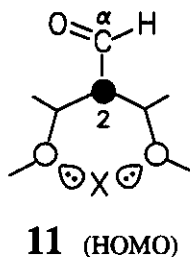
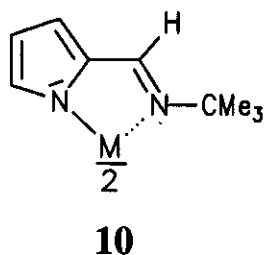


Figure 7. Reduced ^1H nmr shifts δ of a) **9a** (Co) and b) **9b** (Ni) in $\text{C}_2\text{D}_2\text{Cl}_4$ or in CDCl_3 (filled symbols) as functions of the temperature

DISCUSSION

It may have come as a surprise from Tables 1 - 3 that most of the bonding details are almost indistinguishable in the tetrahedral, diamagnetic or paramagnetic spiroheterocycles (**9a-d**), and also similar to those in the planar Pd complex (**9e**). Hence it appears that use of the *same* chelating ligand (**8**) provides for an optimal situation if comparisons with quantum-mechanical results are intended. Of course, the coordination spheres spanned by the four nitrogen atoms differ in the characteristic manner (Figures 1 - 5): They correspond indeed closely to those in another complete series³⁴ of tetrahedral bis(chelates) (**10**) ($3d^7 - 3d^{10}$), where the Co(II) and Zn(II) complexes³⁵ were isomorphous, the Ni(II) complex had disordered *tert*-butyl groups,³⁶ and the Cu(II) derivative³⁷ was flattened (dihedral angle 60 or 61°) in the same way as **9c** (Entry 38 in Table 3). Compared with these otherwise quite different bis(chelates), our series (**9a-e**) has the advantage of containing the vinamidines whose local symmetry permits to predict the node properties of their molecular orbitals easily. Thus the highest occupied π orbital (HOMO, **11**) carries a non-zero coefficient at C(2) which accounts for π donation into the formyl group. However, the lowest unoccupied π orbital (LUMO, **12**) is shown to have a node at C(2) which precludes its interaction with the formyl substituent attached at this position. Therefore, "back-donation" from the metal-centered orbitals with π symmetry into this LUMO cannot extend into the formyl group. Due to such "filtering", the $p_\pi-d_\pi$ donor or acceptor effects (if any) of the metal cations should emerge more clearly, provided that criteria related to a substituent at C(2) are used (conformation, ir, nmr, or rotation).



To keep matters on scale, we need to have a 2-formylvinamidine reference compound of similar shape where X in **11/12** (or in **4a**) is not a metal ion. The 2,3-dihydro-1,4-diazepinium cation (**7a**) was deemed to be a good model because its *N-N* "bite" distance is only $\approx 10\%$ too long. These "bites" would be much too short in pyrimidinium derivatives ($X = CR_2$)³⁸⁻⁴⁰ as well as in dihydro-1,3,2-diazaborinines⁴¹⁻⁴³ ($X = BR_2$). By comparison of **9a-e** in Table 4 with the reference compound (**7a**) we have seen that ir intensities (Entry 49) provide unsuitable criteria, whereas ir wavenumbers (Entry 48) show the enhanced π donation in **9a-e** but do not differentiate between the metal ions.

Our X-ray structural analyses (Figures 1 - 5) revealed the general tendency in **9a-e** to keep the formyl substituent coplanar with the vinamidine, as expected from **4c**; but the π donation was not expressed by changes in the bond distances C(4)-O or C(2)-C(4). However, the activation enthalpies ΔH^\ddagger in Table 4 (Entry 50) demonstrate that formyl rotation occurs most easily at the vinamidinium moiety of **7a**, more slowly in **9b** (Ni), and with the highest energy demand at the stronger π -donating vinamidinide systems of Zn (**9d**) and Pd (**9e**). Relative to benzaldehyde with $\Delta H^\ddagger = 8.3(2)$ kcal/mol,⁴⁴ the formyl rotation in **7a** is electronically impeded

by 4 kcal/mol. This sets a lower limit for the energetic π -donor effect of vinamidinium since the coplanar ground state of **7a** should be destabilized owing to the steric repulsion caused by the seven-membered ring. Vinamidinium is also a stronger donor than 4-Me₂NC₆H₄ in 4-dimethylaminobenzaldehyde in which formyl rotation occurs with $\Delta H^\ddagger = 11.0^{45}$ or $10.3(3)^{46}$ kcal/mol. The effects are reasonably larger in the metal complexes (Entry 50); conversely, the π -electron pressure from vinamidine to the metal ion is the second factor²¹ determining the 3d-orbital sequence with two degenerate SOMOs.

Activation entropies ΔS^\ddagger (Entry 52 of Table 4) could not be obtained for **9a** (Co) and with low precision only for **9b** (Ni); but the slightly positive values for **7a**, **9d** (Zn) and **9e** (Pd) agree well with those of benzaldehyde ($+3.6 \pm 1.2$)⁴⁴ and of 4-dimethylaminobenzaldehyde ($+1.7^{45}$ or -0.8^{46}). It is therefore reasonable to assume similar activation entropies for **7a** and **9a-e**, such that the ΔG^\ddagger data may also be used for energetic comparisons. On this basis (Entry 54), formyl rotation in **7a** is again more expensive by 3.3 kcal/mol than in benzaldehyde ($\Delta G^\ddagger = 7.7^{29,44,45}$) and by 0.4 kcal/mol than in 4-dimethylaminobenzaldehyde ($\Delta G^\ddagger = 10.6^{45,46}$). The closed-shell bis(chelates) (**9d**) (tetrahedral Zn) and (**9e**) (planar Pd) rotate with a barrier of ≈ 15.6 kcal/mol, while the tetrahedral open-shell complexes (**9a**) (Co) and (**9b**) (Ni) require only ≈ 14.7 kcal/mol. If the latter difference of ≈ 0.9 kcal/mol can be ascribed mainly to electron transfer from the HOMO (**11**) to the two 3d holes in **9b** ($3d^8$), it follows that this p_π - d_π bonding effect is energetically quite small, as discussed recently.⁴⁷ It could be even zero for the third 3d hole in **9a** (Co, $3d^7$), suggesting that the additional unpaired electron might perhaps reside in an orbital with symmetry properties different from **11**.

EXPERIMENTAL

Melting points are uncorrected. Ir: IFS-45 (Bruker); uv/vis: PRQ 20 (C. Zeiss); ¹H nmr: WP-80-CW and AW-80 (Bruker), HA-60-IL and VXR-400S (Varian); ¹³C nmr: VXR-400S and XL-100 (Varian), WP-80-DS (Bruker). All nmr chemical shifts δ were referenced to internal TMS. ¹H-Nmr shifts δ_T of the paramagnetic complexes (**9a**) and (**9b**) were measured at variable temperatures T (K) in 1,2-dideuterio-1,1,2,2-tetrachloroethane (C₂D₂Cl₄, $\delta = 5.91$) at 60 Mz (HA-60); they were converted^{32,33} into reduced shifts $\vartheta = (\delta_{Zn} - \delta_T) \cdot T / (298 \text{ K})$ where δ_{Zn} is the corresponding shift in **9d**. Temperatures T in the nmr spectrometer were determined with methanol and glycol tubes or with a non-magnetic chromel-alumel thermocouple (Philips) positioned at the height of the transmitter coil in a nmr tube filled with C₂H₂Cl₄.

[2-(Dimethylaminomethylene)propane-1,3-diyldene]bis(dimethylammonium perchlorate) (**5**) may be prepared in large batches from 0.6 mol of bromoacetic acid as specified,¹⁰ with slight modifications.⁴⁸

N,N'-Bis(3,5-dimethylphenyl)-1,2-ethanediamine (6a) and Bis(hydrochloride). 1,2-Dibromoethane (1.93 ml, 22.4 mmol) in 43.7 ml (350 mmol) of 3,5-dimethylaniline was heated with stirring under Ar at 100°C for 110 min. The product was dissolved in CH₂Cl₂ (150 ml) and distilled water (200 ml). The separated CH₂Cl₂ layer was washed with water (4 x 200 ml), dried with Na₂SO₄, and concentrated. 3,5-Dimethylaniline (27.2 g) was distilled off at 55-80°C/0.1 Torr. The viscous residue was dissolved in 30 ml of methanol, cooled in ice, and treated with 10 ml of concentrated HCl. After 12 h at room temperature the precipitated bis(hydrochloride) of **6a** was isolated by suction, washed with 10 ml of ethanol, and dried to give 5.89 g (77 %) of a colorless powder. Threefold recrystallization from anhydrous ethanol afforded thin platelets decomposing at 216-226°C: Ir (KBr) $\nu = 2917, 2800\text{-}2400$ (N-H), 1563 cm^{-1} ; uv (DMSO) λ_{max} (lg ϵ) = 260 (4.369), 301

(3.683) nm; ^1H nmr (DMSO- d_6) δ = 2.24 (s, 4 CH_3), 3.50 (s, 2 CH_2), 6.82 (s, 2 p -H), 6.92 (s, 4 o -H), 9.93 (br s, 4 NH). Anal. Calcd for $\text{C}_{18}\text{H}_{26}\text{N}_2\text{Cl}_2$: C, 63.34; H, 7.68; N, 8.21. Found: C, 63.21; H, 7.76; N, 8.32. - This crude bis(hydrochloride) (3.00 g, 8.79 mmol) was converted into the free base (**6a**) by shaking with a mixture of CH_2Cl_2 and 2 N NaOH, yielding 2.21 g (94%) of crude **6a** with mp 62-64°C: ^1H Nmr (CCl_4) δ = 2.16 (s, 4 CH_3), 3.23 (s, 2 CH_2), 3.53 (s, 2 NH, exchangeable with D_2O), 6.09 (s, 4 o -H), 6.23 (s, 2 p -H).

6-Formyl-2,3-dihydro-1,4-bis(3,5-dimethylphenyl)-1,4-diazepinium Perchlorate (7a). The diamine (**6a**) (1.34 g, 5.0 mmol) was almost completely soluble in 15 ml of ethanol (99%). After addition of 1.91 g (5.0 mmol) of the bis(perchlorate) (**5**), the suspension was stirred during the slow introduction of aqueous HClO_4 (70%, 1.44 g, 10.0 mmol). Heating to 100°C under N_2 at a reflux condenser for 5 h caused slow dissolution of the salts. Yellow needles deposited from the brown solution on standing at 25°C for 24 h. They were washed with ethanol (99%, 20 ml) and dried to yield 2.02 g (93%) of cannula-shaped crystals with mp 223-225°C after bursting (by occluded ethanol?) at 130-140°C. The mother liquor contains dimethylammonium perchlorate and should be discarded; the excess of HClO_4 served to protect **7a** from decomposition³ by alkali.

The analytical sample, obtained after recrystallization from anhydrous ethanol and drying, had to be heated as a powder to 100°C (oil bath and safety shield!) at 0.001 Torr for 10 h to remove traces of ethanol; mp 227-227.5°C: Ir (KBr) ν = 3020, 2960, 2925, 2860 (w), 1695 (C=O), 1622 (s), 1559 (s), 1096 (s, ClO_4) cm^{-1} ; uv (MeCN) λ_{max} (lg ϵ) = 263 (4.232), 372 (4.393) nm; ^1H nmr (acetone- d_6 /DMSO- d_6 5:1, +21°C) δ = 2.41 (s, 4 CH_3), 4.72 (br¹⁴ s, 2 CH_2), 7.21 (s, 2 p -H), 7.35 (s, 4 o -H), 8.72 (s, 5-/7-H), 9.72 (s, formyl-H); ^{13}C nmr (acetone- d_6 /DMSO- d_6 5:1, +25°C) δ = 21.1 (qt, 1J = 127.0 Hz, 4 CH_3), 57.6 (tm, 1J = 149 Hz, C-2/-3), 109.1 (dt, 2J = 24.8 Hz, 2J = 2.5 Hz, C-6), 121.5 (dq, 1J = 162 Hz, 2J = 5 Hz, 4 o -C), 131.5 (dm, 1J = 158 Hz, 3J = 5 Hz, 2 p -C), 140.6 (q, 2J = 6 Hz, 4 m -C), 146.4 (s, 2 i -C), 159.8 (dm, 1J = 175 Hz, C-5/-7), 189.2 (dt, 1J = 182.3 Hz, 3J = 4.6 Hz, C- α). ^1H -Nmr lineshape analyses (80 and 400 MHz): $\Delta\delta$ = 0.43 for 5-/7-H down to -61°C. Anal. Calcd for $\text{C}_{22}\text{H}_{25}\text{N}_2\text{O}_5\text{Cl}$: C, 61.04; H, 5.82; N, 6.47. Found: C, 61.07; H, 5.91; N, 6.47.

6-Formyl-2,3-dihydro-1,4-diphenyl-1,4-diazepinium Perchlorate (7b). Commercial 1,2-dianilinoethane (**6b**, 5.30 g, 25 mmol) was treated as described above for **7a** with **5** (9.55 g, 25 mmol) and HClO_4 (7.20 g, 50 mmol). The crude product (8.92 g, 95%) was recrystallized once from anhydrous ethanol/acetonitrile (1:1) to afford brown-yellow crystals with mp 273.5-274°C (decomp.) which were always twinned but did not retain ethanol. Ir (KBr) ν = 3060, 1693 (C=O), 1622 (s), 1556 (s), 1097 (s, ClO_4) cm^{-1} ; uv (MeCN) λ_{max} (lg ϵ) = 261 (4.252), 367 (4.379) nm; ^1H nmr (DMSO- d_6) δ = 4.56 (br¹⁴ s, 2 CH_2), 7.60 (s, 2 C_6H_5), 8.64 (s, 5-/7-H), 9.63 (s, formyl-H). Anal. Calcd for $\text{C}_{18}\text{H}_{17}\text{N}_2\text{O}_5\text{Cl}$: C, 57.38; H, 4.55; N, 7.43. Found: C, 57.31; H, 4.56; N, 7.49.

3-(3,5-Dimethylphenylamino)-2-(dimethylphenyliminomethyl)propenal (8). A 250-ml 3-necked flask with reflux condenser and a mechanical stirrer was charged with ethanol (99%, 120 ml) and the bis(perchlorate) (**5**) (22.9 g, 60 mmol). Perchloric acid (70% HClO_4 , 10.3 ml, 120 mmol) was added slowly with stirring, followed by 14.6 g (120 mmol) of 3,5-dimethylaniline. Product formation started quickly at the surface of undissolved **5** and was completed by stirring and heating to 105°C for 90 min. The yellow hydrogenperchlorate of **8** was isolated by suction, washed with 99% ethanol, and dried: 24.1 g (99%), mp 213-214°C (lit.,⁶ mp 216-217°C).

This material was shaken with 2 N NaOH/ CH_2Cl_2 to give the free base (**8**) which was crystallized from cy-

clohexane: mp 148-150°C (lit.,⁶ mp 153-154.5°C). ¹H Nmr (CCl₄) δ = 2.30 (s, 4 CH₃), 6.65 (s, 6 aromat. H), 8.12 (br s, 2 CHN), 9.15 (s, formyl-H), ≈11.5 (very br s, NH); ¹³C nmr (CDCl₃ at -30°C) δ = 21.4 (4 CH₃), 109.9 (C-2), 115.4 and 118.2 (2 x 2 *o*-C), 127.2 and 127.7 (2 x 1 *p*-C), 138.9 and 139.6 (2 x 2 *m*-C), 140.4 and 148.3 (2 x 1 *i*-C), 153.1 and 153.5 (C-1/-3), 188.7 (C-α); ¹³C nmr (CDCl₃ at +28°C) δ = 21.1, 110.3, 117.1 (br, *o*-C), 127.4, 139.2, no *i*-C (br), 153.4, 188.2.

General Procedure for the Preparation of Chelate Complexes (9). Sodium (690 mg, 30 mmol) was dissolved completely in anhydrous ethanol (30 ml) at a reflux condenser under Ar. With stirring of the warm solution, the solid 8-hydrogenperchlorate (4.07 g, 10 mmol) was added batchwise. The resulting yellow suspension was kept warm and combined with 7.6 mmol of one of the divalent metal salts in the following way: Cobalt or nickel acetate (tetrahydrates) added dropwise as hot solutions in anhydrous ethanol (30 ml), but bis-(tetraethylammonium) tetrahalocuprate^{49,50} or the zincate^{49,50} and also bis(benzonitrile)palladiumdichloride^{51,52} added as solids. Chelate formation started immediately with coloring but had to be completed by heating to 105°C (bath temp.) for 3 - 4 h. After slow cooling to room temperature, the precipitated complexes were collected on a small funnel by mild suction and washed in the following sequence: Twice with 99% ethanol, twice with distilled water to remove ethanol and salts, twice with aqueous (99:1) acetic acid (until weakly acidic) to dissolve residual ligand and basic metal(II) salts, twice with water until neutral, and finally with 99% ethanol. In order to minimize thermal decomposition, the dried and recrystallized samples were inserted into the hot block (200°C) for determination of the melting points.

Bis{N-[3-(3,5-dimethylphenylimino)-2-formyl-1-propenyl]-3,5-dimethylanilinato-N,N' }cobalt(II) (9a).

With Co(O₂CCH₃)₂·4 H₂O (1.89 g, 7.6 mmol), the general procedure gave bright orange cubes (2.18 g, 65%) with mp 240-243°C. Threefold recrystallization from anhydrous ethanol (60 ml/g) raised the mp to 248-250°C (decomp.). Ir (KBr) ν = 2920, 2860, 2730 (w, CHO), 1663 (C=O), 1596, 1572 (s), 1499 (s), 1324 (s), 1217 cm⁻¹; uv (dioxane) λ_{max} (lg ε) = 284 (4.593), 369 (4.521), 465 (sh, 3.474) nm; ¹H nmr (C₂D₂Cl₄ at +28°C) δ = -15.5 and -14.3 (1 + 1 *p*-H), -5.7 (4 CH₃), +18.0 (formyl-H), +452 (extremely br., 1/-3-H), rest not observed; coalescence at +32 (±2)°C and 60 MHz for *p*-H with the rate constant k_c = 169 s⁻¹. Anal. Calcd for C₄₀H₄₂N₄O₂Co: C, 71.74; H, 6.32; N, 8.37. Found: C, 71.32; H, 6.10; N, 8.31.

Bis{N-[3-(3,5-dimethylphenylimino)-2-formyl-1-propenyl]-3,5-dimethylanilinato-N,N' }nickel(II) (9b).

Dark red needles (1.71 g, 51%) were obtained by application of Ni(O₂CCH₃)₂·4 H₂O (1.90 g, 7.6 mmol) in the general procedure; mp 258-260°C (decomp.) after one recrystallization from anhydrous ethanol (60 ml/g). Ir (KBr) ν = 2918, 2865, 2735 (w, CHO), 1664 (C=O), 1596, 1577 (s), 1501 (s), 1320 (s), 1221 cm⁻¹; uv (dioxane) λ_{max} (lg ε) = 286 (4.642), 358 (4.456), 458 (sh, 3.710), 605 (2.620) nm; ¹H nmr (CDCl₃ or C₂D₂Cl₄ at +26°C) δ = -11.8 (formyl-H), -10.7 and -9.7 (1 + 1 *p*-H), -5.0 and -4.3 (very br., 2 + 2 *o*-H), -2.3 (4 CH₃), +359.0 and +374.4 (extremely br., 1/-3-H); Δν (Hz at 60 MHz) and rate constants k_c (s⁻¹) at the coalescence temperatures (T_c - 273 K): CH₃ 19 Hz and 42 s⁻¹ at +13 (±2)°C, *p*-H 65 Hz and 144 s⁻¹ at +30 (±2)°C, 1/-3-H 751 Hz and 1667 s⁻¹ at +60 (±5)°C. Anal. Calcd for C₄₀H₄₂N₄O₂Ni: C, 71.76; H, 6.32; N, 8.37. Found: C, 71.91; H, 6.02; N, 8.38.

Bis{N-[3-(3,5-dimethylphenylimino)-2-formyl-1-propenyl]-3,5-dimethylanilinato-N,N' }copper(II) (9c).

Halved amounts in the general procedure, using bis(tetraethylammonium) tetrachlorocuprate(II)^{49,50} (1.77 g, 3.8 mmol), afforded crude 9c (1.65 g, 98%). After twofold recrystallization from anhydrous ethanol (120 ml/g), the dark green needles had mp 264-264.5°C (decomp.). Ir (KBr) ν = 2918, 2862, 2730 and 2710 (w,

CHO), 1666 (C=O), 1598, 1576 (s), 1505 (s), 1323, 1220 (s) cm^{-1} ; uv (dioxane) λ_{max} (lg ϵ) = 295 (4.671), 382 (4.570), 655 (very br., 3.223) nm; ^1H nmr (CDCl_3) extremely br. (≈ 15 ppm) centered at $\delta = -3$ ppm. Anal. Calcd for $\text{C}_{40}\text{H}_{42}\text{N}_4\text{O}_2\text{Cu}$: C, 71.24; H, 6.28; N, 8.31. Found: C, 71.04; H, 6.23; N, 8.11.

Bis(*N*-[3-(3,5-dimethylphenylimino)-2-formyl-1-propenyl]-3,5-dimethylanilinato-*N,N'*)zinc(II) (9d). Application of bis(tetraethylammonium) tetrabromozincate(II)^{49,50} (4.91 g, 7.6 mmol) in the general procedure gave 2.78 g (82%) of bright yellow 9d with mp 229-233°C. The shining, block-shaped crystals obtained by twofold recrystallization from anhydrous ethanol/ethyl acetate (3:2) had mp 233-234°C (decomp.). Ir (KBr) $\nu = 2919, 2852, 2733$ (w, CHO), 1663 (C=O), 1598, 1577 (s), 1508 (s), 1326, 1219 cm^{-1} ; uv (dioxane) λ_{max} (lg ϵ) = 291 (4.656), 382 (4.649) nm; ^1H nmr (CDCl_3 or $\text{C}_2\text{D}_2\text{Cl}_4$ at +32°C) $\delta = 2.20$ (s, 4 CH_3), 6.47 (s, 4 *o*-H), 6.75 (s, 2 *p*-H), 8.02 and 8.60 (2 very br s, 1-*f*-H), 9.29 (s, formyl-H). ^1H -Nmr lineshape analyses (80 MHz): $\Delta\delta = 0.562 + 0.00068 \cdot (T - 273 \text{ K})$ for 1-*f*-H down to -49°C. Anal. Calcd for $\text{C}_{40}\text{H}_{42}\text{N}_4\text{O}_2\text{Zn}$: C, 71.05; H, 6.26; N, 8.29. Found: C, 71.42; H, 6.24; N, 8.39.

Bis(*N*-[3-(3,5-dimethylphenylimino)-2-formyl-1-propenyl]-3,5-dimethylanilinato-*N,N'*)palladium(II) (9e). Use of bis(benzonitrile)palladiumdichloride^{51,52} with halved amounts of the general procedure yielded 1.74 g (97%) of crude 9e. The red, block-shaped crystals obtained after threefold recrystallization from anhydrous ethanol/ CHCl_3 (2:5) had mp 242-243°C (decomp.). Ir (KBr) $\nu = 2917, 2862, 2712$ (w, CHO), 1658 (C=O), 1600, 1579 (s), 1510 (s), 1326, 1230, 1146, 842 cm^{-1} ; uv (CHCl_3) λ_{max} (lg ϵ) = 313 (4.636), 411 (4.131) nm; ^1H nmr (CDCl_3 or $\text{C}_2\text{D}_2\text{Cl}_4$ at +31°C) $\delta = 2.19$ (s, 4 CH_3), 6.50 (s, 4 *o*-H), 6.60 (s, 2 *p*-H), 7.15 and 7.47 (2 very br s, 1-*f*-H), 9.22 (s, formyl-H). ^1H -Nmr lineshape analyses (80 MHz): $\Delta\delta = 0.40$ for 1-*f*-H down to -31°C. Anal. Calcd for $\text{C}_{40}\text{H}_{42}\text{N}_4\text{O}_2\text{Pd}$: C, 66.99; H, 5.90; N, 7.81. Found: C, 65.63; H, 5.90; N, 8.15.

X-Ray Data Collections and Structural Solutions. Single crystals were obtained by slow cooling (styropore isolation) of the hot, filtered solutions ($\approx 0.01 \text{ M}$) and storing for 1 - 14 days at room temperature in the following solvents: Anhydrous ethanol (9a, 9c); anhydrous ethyl acetate (9b), ethanol/ethyl acetate (2:1) (9d), ethanol/ CHCl_3 (2:5) (9e). All crystals were analyzed at +21 (± 1)°C on an ENRAF-Nonius CAD4 diffractometer, using $\text{Mo-K}\alpha$ radiation ($\lambda = 0.71069 \text{ \AA}$) from a highly oriented graphite monochromator, 2θ range = 4 - 46°, ω scan type, scan range (ω) = 1.00° (or 0.90°) + $0.35 \cdot \tan\theta$. Empirical absorption corrections (psi-scans) were applied in the cases of 9a and 9b; see Table 5. In spite of almost equivalent axes *a* and *c*, the cells of 9a (Co), 9b (Ni) and 9d (Zn) are not orthorhombic because the intensities were not consistent with an orthorhombic *C*-centered lattice. For 9e (Pd) only the centrosymmetric part of the data was measured.

The structures were solved with direct methods using the Siemens SHELXTL PLUS (VMS) program package; refinements by full-matrix least-squares (2 blocks in the case of 9e), $w(F_o - F_c)^2$ minimized, hydrogen atoms with fixed isotropic *U*, weighting by $w^{-1} = \sigma^2(F_o)$; for further details, see Table 5. Additional tables of thermal parameters, fractional coordinates including hydrogen atoms, and structure factor amplitudes will be deposited under the reference no. CSD-58456 at the Fachinformationszentrum Karlsruhe, Gesellschaft für wissenschaftlich-technische Information m.b.H., D-76344 Eggenstein-Leopoldshafen, Germany.

Infrared Intensities. The solvent 1,1,2,2-tetrachloroethane ($\text{C}_2\text{H}_2\text{Cl}_4$) was purified by extraction with K_2CO_3 solution, then distilled and redistilled with bp 71-73°C/54 Torr in a Vigreux column (15 cm) under N_2 . It had a refraction index $n_D^{20} = 1.4951$ (lit., 1.4940) and no significant ir absorption at 1500-2300 cm^{-1} .

Solutions of 7a and 9a-e were measured at ambient temperature with a spectral resolution of 2 cm^{-1} against the pure solvent, using a NaCl cuvette ($d = 0.0204 \text{ cm}$) and concentrations adjusted for 20-60% transmission. In case of a well-separated absorption band, plotted as $\lg(I_o/I)_v$ versus cm^{-1} , the base line was defined by the two limiting minima; otherwise, the main base line was used. The expanded absorption areas were cut out from a copy, weighed and converted to the integral absorption $K = \int \lg(I_o/I)_v dv$ (in cm^{-1}). With a known concentration *c* (mol/l), the molar integral absorption^{24,25} was obtained as $E = K/(cd)$ in $\text{l}\cdot\text{mol}^{-1}\cdot\text{cm}^{-2}$.

The experimental setup was checked with a 0.045 M solution of ethyl acetate in $\text{C}_2\text{H}_2\text{Cl}_4$, giving $\lg E = 4.187$ in the limits 1670-1790 cm^{-1} . Seth-Paul²⁴ reported $\lg E = 4.053-4.187$ in CCl_4 . For all chelate complexes the

molar intensity data were divided by 2 on account of two carbonyl groups in the molecule; see Table 4 for the further results.

Table 5. Crystallographic data and computational details for X-ray analyses of 9a-e

C ₄₀ H ₄₂ N ₄ O ₂ M, M =	Co (9a)	Ni (9b)	Cu (9c)	Zn (9d)	Pd (9e)
mol. mass (g/mol)	669.73	669.50	674.35	676.18	717.20
crystal size (mm ³)	0.27x0.33 x0.37	0.13x0.20 x0.23	0.17x0.20 x0.47	0.33x0.40 x0.53	0.17x0.33 x0.50
crystal system	monoclinic	monoclinic	orthorhomb.	monoclinic	triclinic
space group (no.)	I 2/a (15)	I 2/a (15)	P bcn (60)	I 2/a (15)	P 1 (1)
a (Å)	15.999(3)	16.038(3)	8.032(2)	15.957(4)	10.039(3)
b (Å)	14.066(3)	13.963(3)	29.883(5)	14.121(3)	11.627(3)
c (Å)	16.007(4)	16.032(4)	15.189(4)	16.013(4)	17.622(5)
α (°)	90.0	90.0	90.0	90.0	108.46(2)
β (°)	91.53(2)	90.58(2)	90.0	91.55(2)	95.78(2)
γ (°)	90.0	90.0	90.0	90.0	111.40(2)
volume (Å ³)	3601(6)	3590(6)	3646(6)	3607(6)	1761(3)
D _{calc} (g cm ⁻³)	1.235	1.239	1.228	1.245	1.351
Z	4	4	4	4	2
μ (mm ⁻¹)	0.511	0.578	0.636	0.733	0.557
absorptn	0.9604	0.8815	none	none	none
correctns	T_{min} 0.9988	0.9962	none	none	none
max mesrg time (s)	120	120	60	120	45
reflectns measured	±h,+k,+l	±h,+k,+l	+h,+k,+l	±h,+k,+l	±h,±k,+l ^a
reflectns collected	3146	3140	2736	3142	5070
unique reflectns	2930	1932	2130	2921	4731
obsvd reflectns	2083	1645	1552	2563	4647
F	4σ(F)	4σ(F)	4σ(F)	4σ(F)	0σ(F)
F(000)	1412	1416	1420	1424	744
GOOF	3.64	2.58	2.77	4.07	2.59
variables	213	213	213	213	844
reflectns/variables	9.8:1	7.7:1	7.3:1	12.0:1	5.5:1
final R	0.0440	0.0388	0.0497	0.0397	0.0385
final R _w , σ ⁻² (F _o)	0.0346	0.0352	0.0319	0.0352	0.0240
max resdl dens, (e Å ⁻³)	+0.34, -0.33	+0.22, -0.25	+0.36, -0.23	+0.28, -0.35	+0.71, -0.48

^a Only the centrosymmetrical part was measured for Pd (9e).

ACKNOWLEDGEMENT

This work has been supported by the *Stiftung Volkswagenwerk*, the *Deutsche Forschungsgemeinschaft*, and the *Fonds der Chemischen Industrie*.

REFERENCES AND NOTES

1. Paramagnetically induced nmr shifts, part 14. - Part 13: F. Ruf, J. Högerl, R. Knorr, and H. Bronberger, *Chem. Ber.*, **1985**, *118*, 4754.
2. D. Lloyd and H. McNab, *Angew. Chem.*, **1976**, *88*, 496; *Angew. Chem., Int. Ed. Engl.*, **1976**, *15*, 459.
3. D. Lloyd, H. P. Cleghorn, and D. R. Marshall, *Adv. Heterocycl. Chem.*, **1974**, *17*, 1.
4. D. Lloyd and H. McNab, *Heterocycles*, **1978**, *11*, 549.
5. A. R. Butler, D. Lloyd, H. McNab, D. R. Marshall, and K. S. Tucker, *Liebigs Ann. Chem.*, **1989**, 133.
6. R. Knorr, F. Ruf, J. Högerl, M. Hilpert, and P. Hassel, *Chem. Ber.*, **1985**, *118*, 4743.
7. H.-W. Wanzlick and W. Löchel, *Chem. Ber.*, **1953**, *86*, 1463.
8. B. Eistert and F. Haupter, *Chem. Ber.*, **1960**, *93*, 264.
9. D. Lloyd, C. Reichardt, and M. Struthers, *Liebigs Ann. Chem.*, **1986**, 1368.
10. Z. Arnold, *Collect. Czech. Chem. Commun.*, **1965**, *30*, 2125.
11. D. Lloyd, K. S. Tucker, and D. R. Marshall, *J. Chem. Soc., Perkin Trans. 1*, **1981**, 726.
12. D. Lloyd, R. K. Mackie, H. McNab, and K. S. Tucker, *Tetrahedron*, **1976**, *32*, 2339.
13. W. Grahn, *Z. Naturforsch., Part B*, **1976**, *31*, 1641.
14. D. Lloyd, R. K. Mackie, H. McNab, and D. R. Marshall, *J. Chem. Soc., Perkin Trans. 2*, **1973**, 1729.
15. R. Allmann and T. Debaerdemaeker, *Cryst. Struct. Commun.*, **1979**, *8*, 445.
16. G. Ferguson, W. C. Marsh, D. Lloyd, and D. R. Marshall, *J. Chem. Soc., Perkin Trans. 2*, **1980**, 74.
17. G. Ferguson, B. L. Ruhl, T. Wieckowski, D. Lloyd, and H. McNab, *Acta Crystallogr., Sect. C*, **1984**, *40*, 1740.
18. G. Ferguson, M. Parvez, D. Lloyd, H. McNab, and D. R. Marshall, *Acta Crystallogr., Sect. C*, **1990**, *46*, 1248.
19. V. Prelog and G. Helmchen, *Angew. Chem.*, **1982**, *94*, 614, see Scheme 2 on p. 622 therein; *Angew. Chem., Int. Ed. Engl.*, **1982**, *21*, 567.
20. W. C. Lin and L. Orgel, *Mol. Phys.*, **1964**, *7*, 131.
21. A. Ceulemans, M. Dendooven, and L. G. Vanquickenborne, *Inorg. Chem.*, **1985**, *24*, 1153.
22. F. H. Allen, O. Kennard, D. G. Watson, L. Brammer, A. G. Orpen, and R. Taylor, *J. Chem. Soc., Perkin Trans. 2*, **1987**, S1.
23. A. R. Katritzky and R. D. Topsom, *Chem. Rev.*, **1977**, *77*, 639.
24. W. A. Seth-Paul, *Spectrochim. Acta, Part A*, **1974**, *30*, 1817.
25. J. Fruwert and G. Geiseler, *Z. Chem.*, **1980**, *20*, 157.
26. R. N. Jones, D. A. Ramsay, D. S. Keir, and K. Dobriner, *J. Am. Chem. Soc.*, **1952**, *74*, 80.
27. J. P. Collman, *Angew. Chem.*, **1965**, *77*, 154; *Angew. Chem., Int. Ed. Engl.*, **1965**, *4*, 132.
28. R. N. Jones, W. F. Forbes, and W. A. Mueller, *Can. J. Chem.*, **1957**, *35*, 504.
29. F. A. L. Anet and M. Ahmad, *J. Am. Chem. Soc.*, **1964**, *86*, 119.
30. For the method and references, see R. Knorr and A. Schnegg, *Chem. Ber.*, **1979**, *112*, 3515.
31. A. Weiß, *Doctoral Dissertation*, University of Munich, **1976**, p. 128 (in German).
32. R. Knorr, H. Polzer and E. Bischler, *J. Am. Chem. Soc.*, **1975**, *97*, 643.
33. R. Knorr and A. Weiß, *Chem. Ber.*, **1981**, *114*, 2104.
34. R. H. Holm, A. Chakravorty, and L. J. Theriot, *Inorg. Chem.*, **1966**, *5*, 625.
35. C. H. Wei, *Inorg. Chem.*, **1972**, *11*, 1100.
36. C. H. Wei and J. R. Einstein, *Acta Crystallogr., Sect. B*, **1972**, *28*, 2591.
37. C. H. Wei, *Inorg. Chem.*, **1972**, *11*, 2315.
38. G. Ferguson, B. Kaiter, D. Lloyd, and H. McNab, *J. Chem. Res.*, **1984**, S 182, M 1738.
39. G. Ferguson, B. Kaiter, D. Lloyd, and H. McNab, *J. Chem. Res.*, **1984**, S 184, M 1760.
40. G. A. Reynolds, G. H. Hawks, and K. H. Drexhage, *J. Org. Chem.*, **1976**, *41*, 2783.
41. N. Kuhn, A. Kuhn, M. Speis, D. Bläser, and R. Boese, *Chem. Ber.*, **1990**, *123*, 1301.
42. E. Hohaas, *Z. Anorg. Allg. Chem.*, **1982**, *484*, 41.
43. K. Hartke, B. Krug, and R. Hoffmann, *Liebigs Ann. Chem.*, **1984**, 370.
44. L. Lunazzi, *Tetrahedron Lett.*, **1975**, 1205.
45. T. Drakenberg, R. Jost, and J. Sommer, *J. Chem. Soc., Chem. Commun.*, **1974**, 1011.
46. R. E. Klinck and J. B. Stothers, *Can. J. Chem.*, **1976**, *54*, 3267.
47. M. Gerloch and E. C. Constable, "Transition Metal Chemistry", VCH, Weinheim, 1994.
48. F. Ruf, *Doctoral Dissertation*, University of Munich, **1983**, p. 213 (in German).
49. N. S. Gill and R. S. Nyholm, *J. Chem. Soc.*, **1959**, 3997.
50. A. Sabatini and L. Sacconi, *J. Am. Chem. Soc.*, **1964**, *86*, 17.
51. M. S. Kharash, R. C. Seyler, and F. R. Mayo, *J. Am. Chem. Soc.*, **1938**, *60*, 882.
52. J. R. Doyle, P. E. Slade, and H. B. Jonassen, *Inorg. Synth.*, **1960**, *6*, 216.